

Vascularization via activation of VEGF-VEGFR signaling is essential for peripheral nerve regeneration

Yohei NISHIDA¹, Yurie YAMADA², Hiroko KANEMARU¹, Atsushi OHAZAMA³, Takeyasu MAEDA^{2, 4}, and Kenji SEO¹
¹ Division of Dental Anesthesiology, ² Center for Advanced Oral Sciences, ³ Division of Oral Anatomy, Niigata University Graduate School of Medical and Dental Sciences, 2-5274 Gakkocho-dori, Chuo-ku, Niigata 951-8514, Japan, and ⁴ Faculty of Dental Medicine, University of Airlangga, Surabaya 60132, Indonesia

(Received 11 September 2018; and accepted 28 September 2018)

ABSTRACT

Peripheral nerve injury has been suggested to up-regulate mRNA for the vascular endothelial growth factor (VEGF) which enhances nerve regeneration. VEGF is known to regulate angiogenesis by binding with a specific receptor, the vascular endothelial growth factor receptor (VEGFR). However, little is known about the involvement of VEGF-VEGFR signaling in the nerve regeneration at early stages though previous studies contained a lengthy observation. The present study examined that relationship between angiogenesis and peripheral nerve regeneration at the early stage after nerve transection by focusing on the chronological changes in the expression patterns of VEGF-VEGFR signaling. This study used our previously reported experimental model for nerve regeneration following the transection of the inferior alveolar nerve (IAN) in mice. In a double staining of PGP9.5 and CD31, respective markers for the nerve fibers and endothelial cells, CD31 immunoreactions first appeared in the injury site on postoperative (PO) day 2 when the transected nerve fibers had not been re-connected. The most intense immunoreaction for CD31 was found around the regenerating nerve fibers extending from the proximal stump on PO day 3, but it gradually lessened to disappear by PO day 7. The expression patterns of VEGFR1 and VEGFR2 showed similar chronological changes through the observation periods, with most intense immunoreaction found on PO day 3. Western blotting of total protein extracted from the injury site demonstrated the clear bands for VEGF-A and VEGF-B on PO day 2, indicating a time lag for the expression of ligands and receptors. A local administration of antibody to VEGF-A inhibited the elongation of the nerve fibers from the proximal stump. Furthermore, this administration of VEGF-A antibody inhibited the expression of CD31 in the gap between proximal and distal stumps. These results indicated that a nerve injury initiates productions in VEGF-A and VEGF-B, followed with the expression of VEGFR1 and VEGFR2 at early stages after the nerve injury. Taken these findings together, it is reasonable to postulate that immediate response of VEGF-VEGFR signaling to nerve injury plays a crucial role in local angiogenesis, resulting in a trigger for the regeneration of the nerve fibers in mouse IAN.

Address correspondence to: Dr. Kenji Seo
Division of Dental Anesthesiology, Niigata University
Graduate School of Medical and Dental Sciences, 2-5274,
Gakkocho-dori, Chuo-ku, Niigata 951-8514, Japan
Tel: +81-25-227-2970, Fax: +81-25-227-0812
E-mail: seo@dent.niigata-u.ac.jp

Vascular endothelial growth factor (VEGF), a secreted glycoprotein, regulates vascular development in embryo and blood vessel formation during mature period (2, 21). It is categorized as five molecules including VEGF-A, -B, -C, -D and placenta growth factors. Their biological actions are mediated when they bind vascular endothelial growth factor recep-

tor (VEGFR). The VEGFR family mainly consists of three protein-tyrosine kinases including VEGFR1 (also called Flt-1 in mice), VEGFR 2 (called Flk-1) and VEGFR 3. The active receptors initiate signal transduction pathways (10). Signaling is modulated through co-receptors such as heparan sulfate, neuropilins (NPs) and integrins (3). VEGF-A can bind VEGFR1, VEGFR2, NP-1 and NP-2, while VEGF-B binds VEGFR1 and NP-1. These signal pathways via VEGFR1 and -2 have different functions; VEGFR2 is required for endothelial cell function and survival of blood vessels whereas VEGFR1 serves for the recruitment of hematopoietic precursors and monocyte/macrophage migration (14).

Peripheral nerve injury induces Wallerian degeneration at the distal stump (6), the site of occurrence for discontinuation of the nerve trunk, and for the disturbance of blood and nutrition supply. In such a nerve injured site, hypoxia induced by nerve injury causes Schwann cell migration in order to guide the injured nerve fibers across a bridge of regenerating nerve ends. A series of this phenomenon is mediated by VEGF-A, which macrophage secretes (4). In addition, neuronal progenitor cells lacking VEGF-A result in defects of the brain vascularization and neuronal apoptosis (12). Observation of mice lacking VEGF-B showed impaired nerve repair, leading a hypothesis that VEGF-B is also a key molecule for nerve regeneration (6). Clinically, reestablishment of microvascular circulation in the nerve injured site is well-known as a crucial factor which determines a prognosis for recovery of lost sensation (8).

Additional factors have been reported to accelerate angiogenesis within artificial nerve conduit reconnecting nerve gaps, essential for the functional recovery of injured peripheral nerve (9, 13, 15). Although these reports have suggested the involvement of VEGF-VEGFR signaling pathway in nerve regeneration, little information is available regarding early changes in expression patterns of each factor and receptor after peripheral nerve injury. Therefore, this study was undertaken to examine changes in the expression pattern of VEGF/VEGFR system in the regeneration process immediately after artificial nerve transection. Hence, we focused on: 1) the relationship of nerve regeneration and blood vessels; 2) the chronological changes in the expression profile of VEGFR1 and VEGFR2 as well as their ligands including VEGF-A and VEGF-B; and 3) the effect of an antibody to VEGF-A on the regeneration of the nerve fibers. Since our previous study using the same experimental model reported that the transect-

ed nerve fibers of the inferior alveolar nerve (IAN) in mice could be re-connected until postoperative (PO) day 7 (20), the observation periods were determined at the comparatively early stage including at 6 h after nerve injury and from PO days 1 to 7.

MATERIALS AND METHODS

All animal experiments were reviewed and approved by the Niigata University Institutional Animal Care and Use Committee prior to the study (approval number #235-1). The animals were housed in a temperature-controlled room under normal 12 h light/12 h dark laboratory conditions with free access to chow and water.

Animals and nerve transection. This experimental study used 80 male C57BL/6J mice (8–12 week-old) (Charles River Laboratories Japan, Inc., Yokohama, Japan). The transection of the IAN was performed according to a method described previously (20). Briefly, under deep anesthesia with inhalation of sevoflurane and an intraperitoneal injection of 4% chloral hydrate (400 mg/kg), IAN was exposed in the mandibular canal by removing the surface of mandibular bone and then it was transected at one side randomly selected. The cut ends of transected IAN were returned into the canal and then the wound was sutured (experimental group, $n = 65$). Fifteen other mice receiving the operation for IAN exposure without nerve transection served as naïve group.

VEGF-antibody administration. An antibody to VEGF-A (AF-493-NA; R&D system, Minneapolis, MN) was dissolved in 0.1 M phosphate buffered saline (PBS) at a final concentration of 0.2 mg/mL. This polyclonal antibody raised in a goat can recognize VEGF₁₆₄, VEGF₁₂₀, and VEGF₁₈₈ of mouse VEGF-A (<https://resources.rndsystems.com/pdfs/datasheets/af-493-na.pdf>). Sixteen mice received a local administration of the antibody to VEGF-A (5 μ L per animal) or physiological saline (5 μ L per animal) into IAN transection area according to a previously described method (20). This antibody administration was performed every day from postoperative (PO) days 1 to 5.

Tissue preparation and immunohistochemistry. Under deep anesthesia with an intraperitoneal injection described above, mice were transcardially perfused with 4% paraformaldehyde at PO 6 h and days 1, 2, 3, 5 and 7. After decalcification with 10% ethylene

Table 1 *The antibody used in this study*

Antibody	Dilution	Supplier	Purpose
VEGF-A	1 : 500	Abcam (Cambridge, UK)	WB
VEGF-B	1 : 300	Abcam (Cambridge, UK)	WB
Actin	1 : 10,000	Sigma-Aldrich (St. Louis, MO, USA)	WB
VEGFR1	1 : 500	Abcam (Cambridge, UK)	IHC
VEGFR2	1 : 100	Abcam (Cambridge, UK)	IHC
CD31	1 : 200	BD Pharmingen (Franklin Lakes, NJ, USA)	IHC
PGP9.5	1 : 1,000	Ultraclone (Wellow, UK)	IHC
FITC anti-rabbit IgG	1 : 300	Vector (Burlingame, CA, USA)	IHC
Texas Red anti-rat IgG	1 : 300	Vector (Burlingame, CA, USA)	IHC
HRP anti-rabbit IgG	1 : 2,000	Cell Signaling Technology (Danvers, MA, USA)	WB
HRP anti-mouse IgG	1 : 2,000	Cell Signaling Technology (Danvers, MA, USA)	WB

WB: Western blotting, IHC; immunohistochemical study

diamine tetra-acetic disodium (EDTA-2Na; Dojindo Laboratories, Kumamoto, Japan), the mandibles including the IAN were sagittally cut at a thickness of 20 μm in a cryostat. Cryostat sections were processed for immunohistochemistry according to our protocol as previously reported (19). After a treatment with 5% normal goat serum (Vector lab., Burlingame, CA) for 1 h at room temperature, the sections were incubated with primary antibodies as shown in Table 1 at 4°C overnight, followed by an incubation with secondary antibodies (see, Table 1) at room temperature for 1 h. The immunostained sections were examined under a fluorescent microscope (Axioimager M1; Carl Zeiss, Oberkochen, Germany).

Measurement of density of VEGFR immuno-positive area. Fluorescent images of VEGFR positive area were captured and saved in a computer. In each specimen ($n = 4$ each; 3 animals at each stage), a positive area was taken from across the width of the nerve injury area to quantify total area of the VEGFR1 or VEGFR2 signals. The signals were analyzed using the free software Image-J (<http://imagej.nih.gov/ij/>). A threshold for positive reaction was set at same value in all sections. The ratio of VEGFR immuno-reactive area to whole nerve area was measured. Then the mean value and standard deviation was calculated as representative data for each day's specimen.

Retrograde tracing by DiI. An additional 12 mice were used for identifying the nerve regeneration in trigeminal ganglion by DiI labelling technique. The animals were divided into three groups ($n = 4$ each group): intact (without any surgical operation), vehicle control (IAN transection with saline-administration) and VEGF antibody groups. Three μL DiI

(Invitrogen, Waltham, MA, USA) was subcutaneously injected in the vicinity of the mental foramen using a Hamilton syringe at PO day 5. These mice were sacrificed 2 days after DiI injection. Statistical comparisons were assessed between each group with one-way analysis of variance (ANOVA). A *P*-value less than 0.05 was considered a significant difference.

Western blotting. The total protein was extracted from either naïve or injured IAN at PO days 1, 3, 5, and 7. A total of 10 μg of total protein was run on 6% or 12% SDS-PAGE gel, and transferred to polyvinylidene difluoride membrane. The membrane was blocked with 5% non-fat dry milk for 1 h at room temperature, then incubated overnight at 4°C with primary antibodies as shown in Table 1. After washing membrane, it was incubated in a horseradish peroxidase (HRP)-conjugated secondary antibody (see, Table 1) for 1 h at room temperature. Immuno-reactive bands were visualized via the enzyme linked chemiluminescence.

RESULTS

Regeneration of blood vessels and nerve fibers after transection of IAN

We examined chronological changes in regeneration of vessels and nerve fibers by a double immunofluorescent staining using antibodies to PGP 9.5 and CD31, markers for nerve fibers and endothelial cells, respectively. No apparent CD31 immunoreaction was recognizable in the nerve injury sites at 6 h after the transection or PO day 1 when a wide gap existed between the proximal and distal stumps (Fig. 1a, b). On PO day 2, the gap appeared to become narrower than previous stages, suggesting the sprouting of

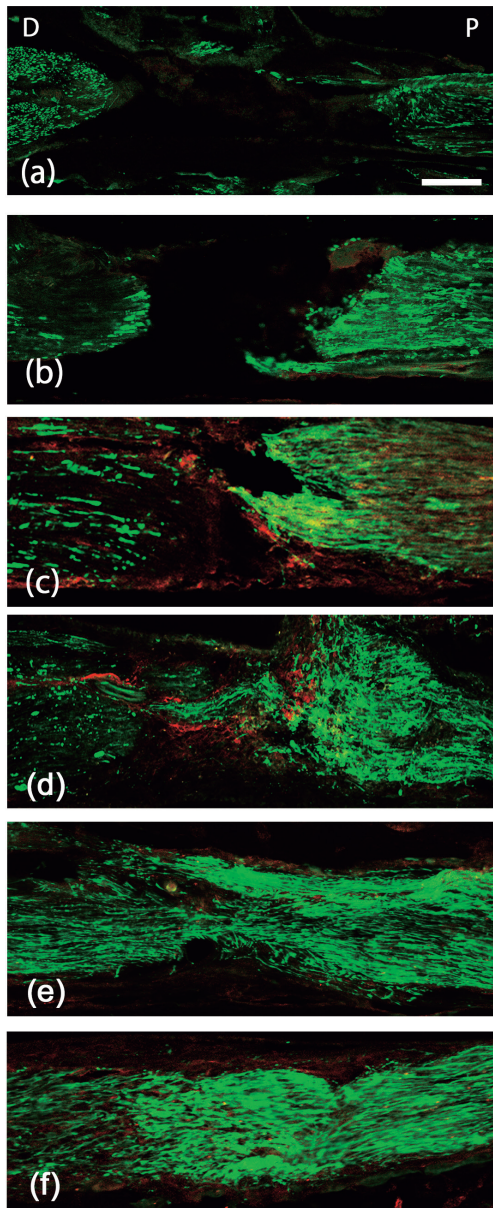


Fig. 1 Double immunofluorescent images showing chronological changes in the distribution of blood vessels and nerve fibers in the mouse inferior alveolar nerve (IAN) on postoperative (PO) 6 h (a), days 1 (b), 2 (c), 3 (d), 5 (e) and 7 (f). PGP9.5 (green)- and CD31 (red)-immunoreactions. No CD31 immunoreaction exists in the nerve injury sites at PO 6 h (a) and day 1 (b), when the nerve sprouting is never seen between the proximal (P) and distal (D) stumps. On PO day 2 (c), the transected nerve fibers are seen to extend from the proximal stump, and many CD31 positive reactions appear in the transected area. The regenerating nerve fibers project from the proximal stump with a concentration of CD31 positive reactions around the regenerating nerve fibers on PO day 3 (d). The nerve fibers elongate extensively from the proximal stump on PO day 5 (e) and to appear to reconnect on PO day 7 (f). However, weak CD31 immunoreactions are sparsely present in and along the IAN bundles. Scale bar indicates 200 μ m. Same magnification in a–f.

the transected nerve fibers from the proximal stump (Fig. 1c). The tips of the proximal stump showed an intense immunoreaction for PGP9.5. Numerous CD31 positive reactions occurred in the transected area, appearing to align in parallel to the nerve fibers. In particular, CD31 positivity appeared densely at the gap between the proximal and distal stumps, where the PGP9.5 positive nerve fibers extended from the proximal stump (Fig. 1c). The nerve bundles both in the proximal and distal stumps also contained CD31 immunoreaction. Furthermore, CD31 immunoreactions were recognizable along the IAN bundles. On PO day 3 when the regenerating nerve fibers projected from the proximal stump more actively, CD31 positive reactions tended to concentrate around these nerve fibers (Fig. 1d). After PO day 5, the nerve fibers with intense PGP9.5 immunoreaction elongated extensively from the proximal stump (Fig. 1e), and the re-connection of the transected nerve fibers appeared to be complete on PO day 7 (Fig. 1f). At these stages, the immunoreaction for CD31 decreased in number and strength; CD31 immunoreactions were sparsely distributed in and along the IAN bundles (Fig. 1e–f).

Expression patterns of VEGFR and VEGF

Immunohistochemical investigations were carried out for investigating chronological alterations in the expression profiles of VEGFR1 and VEGFR2 from PO days 1 to 7. The intact IAN did not exhibit any immunoreaction of VEGFR1 or VEGFR2 except for weak immunoreactions of VEGFR2 along the IAN bundles (Fig. 2Aa, g). In immunohistochemistry for VEGFR1, weak reactions were found in the proximal stump, with the best only faint positivity in the distal stump (Fig. 2Ab). VEGFR1 immunoreactions appeared to become stronger in the IAN, and most intense reactions existed between the proximal and distal stumps on PO days 2 and 3 (Fig. 2Ac, d). However, its immunoreactions tended to gather at the re-connection site with a gradual reduction of immunointensity on PO day 5, with few reactions detectable on PO day 7. VEGFR2 immunohistochemistry demonstrated a similar expression pattern in the regenerating IAN during the observation periods (Fig. 2Ah–l).

Image analysis at the transected area showed that the density of the VEGFR1 immunopositive area increased from PO day 1 ($1.26 \pm 0.25\%$) to PO day 2 ($13.46 \pm 2.77\%$), and reached its maximum on PO day 3 ($24.40 \pm 3.35\%$) (Fig. 2Ba). After PO day 5, the density of immunoreactive area began to fall ($4.20 \pm 0.65\%$), and subsided to an undetectable lev-

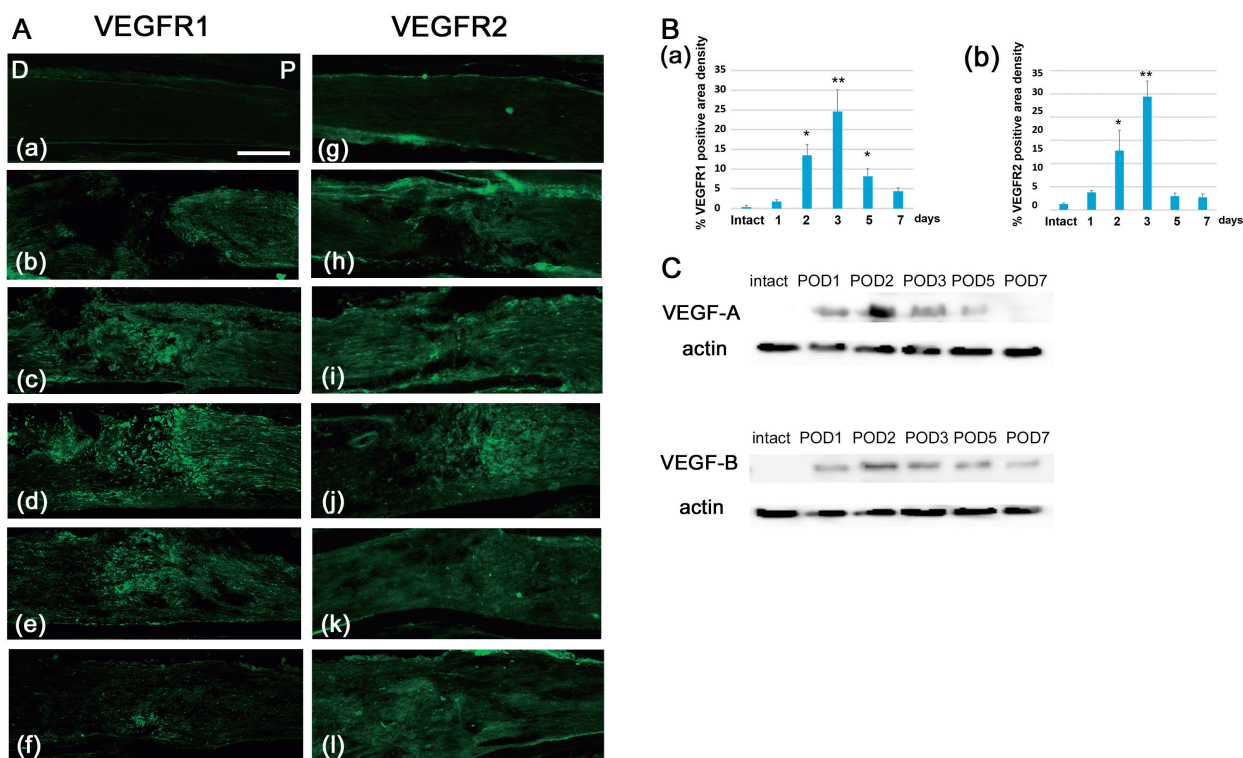


Fig. 2 **A:** Immunofluorescent images showing chronological changes in expression patterns of VEGFR1 (a–f) and VEGFR2 (g–l) in intact mice (a, g), postoperative (PO) days 1 (b, h), 2 (c, i), 3 (d, j), 5 (e, k) and 7 (f, l). VEGFR1 and VEGFR2 demonstrated the same expression patterns throughout the observation periods. Intact animals express neither immunoreaction of VEGFR1 (a) nor VEGFR2 (g). Weak VEGFR1 (b) and VEGFR 2 (h) reactions are observed in the proximal (P) stump whereas faint or no positivity appears in the distal (D) stump. On PO days 2 (c, i) and 3 (d, j), immunoreactions become stronger in the nerve bundles. The immunoreactions show a tendency to concentrate at the reconnection site on PO day 5 (e, k), and gradually weaken on PO day 7 (f, l). Scale bar indicates 200 μ m. Same magnification in all figures. **B:** Bar graphs indicating the density of VEGFR1 (a) and VEGFR2 (b) immunopositive areas. The immunopositive density increases from PO day 1 and reaches its maximum on PO day 3. Asterisks indicate significant differences between intact and experimental animals (*: $P < 0.05$; **: $P < 0.01$). **C:** Western blotting of VEGF-A and VEGF-B during the regeneration of the inferior alveolar nerve (IAN). Both VEGF-A or VEGF-B show apparent increase on PO day 2.

el on PO day 7 ($2.73 \pm 0.74\%$). There were significant differences between intact specimens and PO day 2, between intact specimens and PO day 3, and between intact specimens and PO day 5 (Student's t -test $P < 0.05$, Fig. 2Ba). The density of VEGFR2 positive areas also exhibited similar changes in the expression profiles. The expression of VEGFR2 began to increase from PO day 1 ($3.76 \pm 0.41\%$), reached a peak on PO day 3 ($24.4 \pm 3.45\%$), and decreased thereafter (Fig. 2Bb). There were significant differences between intact specimens and PO day 2, and between intact specimens and PO day 3 (Student's t -test $P < 0.05$, Fig. 2Bb).

In western blotting analysis on VEGF-A and VEGF-B, clear bands for VEGF-A were recognized from PO days 1 to 5 with most intense bands on PO day 2. The antibody to VEGF-A can recognize molecular weights of 23 kDa according to the manufac-

turer's instruction. They began to decrease after PO day 3, and became to undetectable level on PO day 7 (Fig. 2C). The expression of VEGF-B also showed a similar chronological pattern to that of VEGF-A (Fig. 2C).

Effects of neutralizing antibody to VEGF during IAN regeneration

A local administration of an antibody to VEGF-A aimed to investigate the action of VEGF on neural regeneration and angiogenesis in the IAN regeneration model. Since the continuity of nerve fibers was found on PO day 7 as shown in Fig. 1F, we observed the effects of the VEGF-A-antibody on IAN regeneration on PO day 7. In the vehicle control, newly regenerated nerve fibers with PGP9.5 reactions were found in the distal stumps (Fig. 3Aa), appearing similar to the profiles of the nerve fibers in

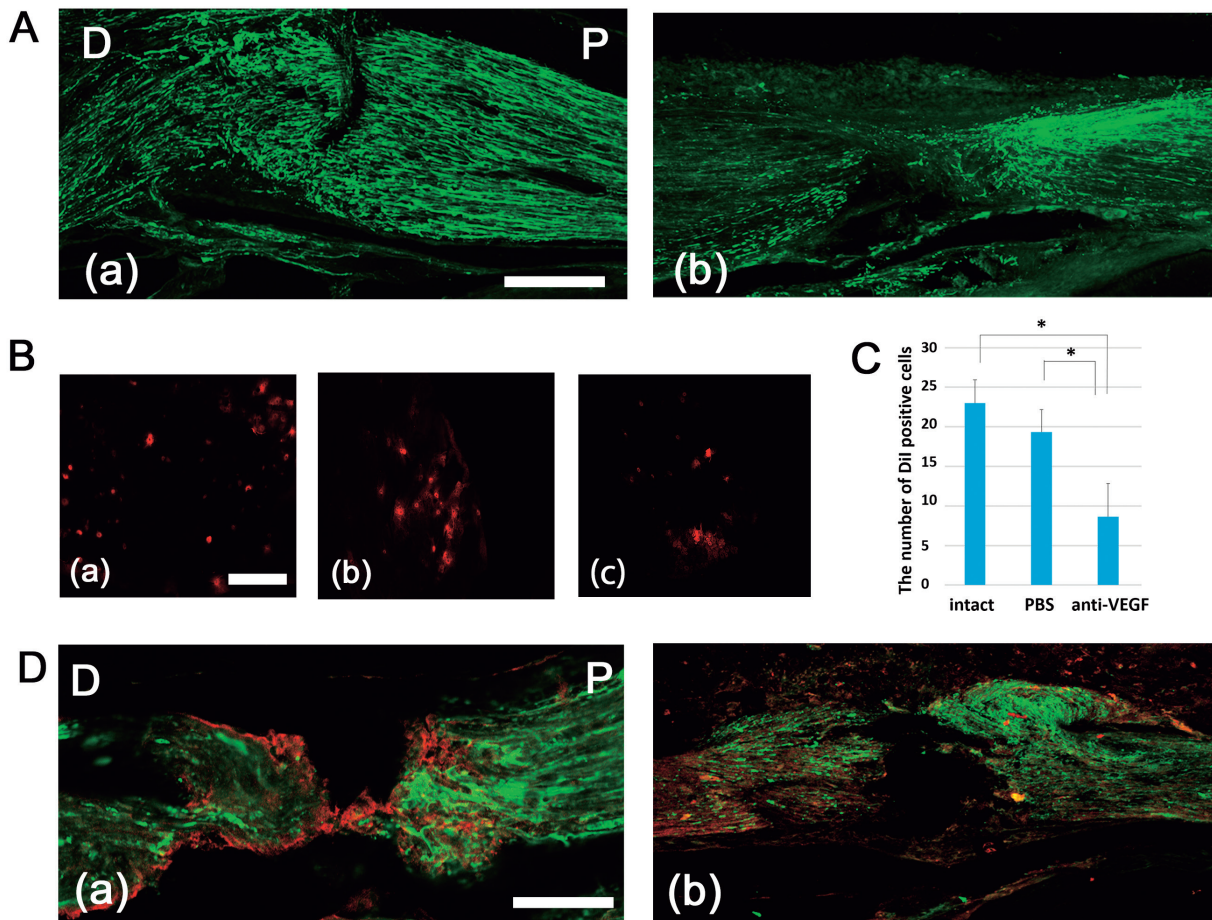


Fig. 3 Effects of a local administration of a neutralizing antibody to VEGF to the transected site of inferior alveolar nerve (IAN). **A:** Immunofluorescent images of a vehicle control (a) and treatment with a neutralizing antibody to VEGF (b) on postoperative (PO) day 7. Immunohistochemical observations of regenerative nerve fibers with PGP9.5 reactions (green) are conducted in longitudinal sections of IAN at PO day 7. The vehicle control group exhibits newly regenerated nerve fibers extending towards the distal (D) from proximal (P) stumps (a) while the administration group shows an inhibition of the neural reconnection (b). Scale bar indicates 200 μ m. Same magnification in a and b. **B:** DiI labelling in the trigeminal ganglion of an intact (a), a vehicle control (b) and treatment with antibody to VEGF-A (c) on PO day 7. More DiI labelled neurons are seen in the vehicle control than administration groups. Scale bar indicates 100 μ m. Same magnification in a, b and c. **C:** A quantitative analysis of the number of DiI labelled trigeminal ganglion neurons. Significant differences exist between the vehicle control and administration groups, and between intact and administration groups (ANOVA, $P < 0.05$). **D:** Immunofluorescent merged images of the vehicle (a) and administration (b) groups on PO day 3. PGP9.5 (green) and CD31 (red) in immunoreactions. The antibody to VEGF-A treatment inhibits CD31 immunoexpression in the space between the proximal (P) and distal (D) nerve stumps. Scale bar indicates 200 μ m. Same magnification in a and b.

the proximal site of IAN (Fig. 3Aa, and see Fig. 1f). An administration of antagonist injection clearly inhibited the reconnection of the PGP9.5 positive nerve fibers (Fig. 3Ab). In addition, a retrograde labelling of DiI tracing was performed to confirm whether newly regenerated nerve fibers in the distal stump have continuity to nerve fibers in the proximal stump. In intact group whose animals received any surgical treatment, DiI tracing technique labelled comparatively large number of trigeminal ganglion neurons (23.0 ± 2.94) (Fig. 3Ba, C). A

smaller number of DiI labelled neurons was found in the trigeminal ganglion in the antibody administered group (Fig. 3Bc) than in the vehicle control group with a PBS injection (Fig. 3Bb). Statistical analysis confirmed that the number of DiI labeled cells in trigeminal ganglion was significantly reduced in the VEGF-A-antibody administrative group (8.66 ± 4.1), compared with those of vehicle control group (19.33 ± 2.86), with a significant difference (one-way ANOVA, $P < 0.05$, Fig. 3C). There was also significant difference between intact and anti-

body-administrative groups (one-way ANOVA, Holm-sidak methods, $P < 0.05$, Fig. 3C). However, no significant difference existed between the intact and vehicle control groups (Holm-sidak methods, $P = 0.32$).

Furthermore, in comparison with control animals (Fig. 3Da), antibody to VEGF-A treatment suppressed CD31 immunoreactivity in the gap between the proximal and distal nerve stumps on PO day 3 (Fig. 3D b). This feature implicated the disturbance of the invasion of endothelial cells positive for CD31 to the gap between the stumps, resulting in a failure of both angiogenesis and elongation of nerve fibers from the proximal stump.

DISCUSSION

Several reports have shown the involvement of VEGF in the peripheral nerve regeneration process after injury. However, since they contained a lengthy observation after axotomy *in vivo* (7, 11, 16, 18), very few reports have been available describing on early changes after nerve injury (4, 6). Current observations by immunostaining and western blotting analyses revealed the most intense expressions of VEGF isoforms—including VEGF-A and VEGF-B—in the transected site of IAN at PO day 2, suggesting the involvement of this molecule in nerve regeneration followed with angiogenesis, as supported by the findings on expression patterns of CD31 immunoreactivity. These findings lead us to the possibility of the existence of a close relationship between neural regeneration and vascularization at the early stage of peripheral nerve regeneration. Thus, we can regard the VEGF-VEGFR signaling pathway as an important cue for peripheral nerve regeneration.

The reestablishment of microvascular circulation is essential for the blood and nutrition/oxygen supply to lesion of damaged nerve fibers during nerve regeneration. In clinics, an artificial nerve or conduit has been using as surgical treatment of nerve injury. Acellular nerve grafts with VEGF used for bridging resected nerve gaps have been reported to induce Schwann cell invasion and neovascularization, but without stimulatory effects on neural outgrowth (7, 17). To overcome this disadvantage for peripheral nerve regeneration, a dual application of nerve growth factor (NGF) and VEGF to the acellular grafts improved motor, nociception, and proprioception functions (9). On the other hand, Sondell *et al.* (1999) revealed the detection of VEGF in dorsal root ganglion (DRG) neurons and the promotion of neural outgrowth by an additional administration of

VEGF (17, 18). These lines of evidences suggest that VEGF has a potential for not only angiogenesis but also nerve regeneration.

The present study was able to demonstrate that the intense expressions of VEGF-A and its receptors appeared prior to the elongation of nerve fibers from proximal nerve end. Following the appearance of VEGF-A and VEGF-B in the injured lesion, the CD31 expression appears to begin from the proximal site towards the distal direction (see, Fig. 1c, d). The disturbance of VEGF by an administration of a neutralizing VEGF-A-antibody clearly inhibited the neural regeneration, implying that VEGF-VEGFR signaling functions in a crucial role for the commencement of nerve regeneration at the early stage of the neural regeneration and vascularization processes. In a previous study, defects of epithelial cells experimentally made in cornea have been shown to require concomitant activation of VEGFR1, VEGFR2, and NP1 for improving sensation and neuronal growth (15). NP, one of the receptors for semaphorin, has also been reported to play a role for nerve fiber guidance (14). Interestingly, NP serves as a co-receptor for VEGF as well as semaphorin—which acts as an inhibitor of neural growth, while VEGF acts as neurotrophic factor (11). In a quantitative study, VEGF has been implicated in the increase in the number of the DRG neurons and motoneurons in addition to that of blood vessels (16). These findings strongly support our notion that VEGF activity on peripheral nerve regeneration consists of two independent activities, including an acceleration of angiogenesis and nerve regeneration.

VEGF-A which binds VEGFR1 and VEGFR2, serves to promote outgrowth of nerve fibers in cultured DRG neurons (21). In contrast, VEGF-B can bind VEGFR1 and NP-1 to play a role in neuroprotection (1). The increased endogenous expression or application of exogenous VEGF-B promotes nerve regeneration without affecting undamaged nerves (6). In addition, VEGF-B has been demonstrated to mediate the nerve regeneration and to restore the sensation and healing responses of peripheral nervous system (6). The present study demonstrated the appearance of VEGF-A and VEGF-B expressions in injured IAN on PO day 2, which coincides with timing for the initial reaction to nerve injury in Wallerian degeneration process. In this period, it has been shown that Schwann cells proliferate within their basal lamina tubes, produce cytokines/trophic factors, and phagocytose detached debris (6). It is, therefore, better to consider that the expression of these receptors in the injured nerves is necessary for

the promotion of neural outgrowth, neuroprotection and angiogenesis, suggesting the adequate timing for initiating nerve regeneration.

In conclusion, this study revealed that transection of IAN induced the expression of VEGF-A and VEGF-B immediately after injury, followed with VEGFR1 and VEGFR2 expression, prior to the commencement of nerve regeneration. An inhibition of VEGF-VEGFR signaling caused a suppression of regenerated neural continuity. Therefore, it is concluded that immediate response of VEGF-VEGFR signaling to nerve injury plays a crucial role in local angiogenesis, resulting in a trigger for the peripheral nerve regeneration.

Acknowledgements

This research was supported by the JSPS KAKENHI (Grant Numbers 15H05041 to K.S., 15K20509 to H.K. and 17H06697 to Y.Y.)

REFERENCES

- Bry M, Kivelä R, Leppänen VM and Alitalo K (2014) Vascular endothelial growth factor-B in physiology and disease. *Physiol Rev* **94**, 779–794.
- Carmeliet P and Storkebaum E (2002) Vascular and neuronal effects of VEGF in the nervous system: implications for neurological disorders. *Semin Cell Dev Biol* **13**, 39–53.
- Claesson-Welsh L (2016) VEGF receptor signal transduction – A brief update. *Vascul Pharmacol* **86**, 14–17.
- Cattin AL, Burden JJ, Van Emmenis L, Mackenzie FE, Hoving JJ, Garcia Calavia N, Guo Y, McLaughlin M, Rosenberg LH, Quereda V, Jamecna D, Napoli I, Parrinello S, Enver T, Ruhrberg C and Lloyd AC (2015) Macrophage-induced blood vessels guide Schwann cell-mediated regeneration of peripheral nerves. *Cell* **162**, 127–139.
- Gaudet AD, Popovich PG and Ramer MS (2011) Wallerian degeneration: gaining perspective on inflammatory events after peripheral nerve injury. *J Neuroinflammation* **8**, 110.
- Guaiquil VH, Pan Z, Karagianni N, Fukuoka S, Alegre G and Rosenblatt MI (2014) VEGF-B selectively regenerates injured peripheral neurons and restores sensory and trophic functions. *Proc Natl Acad Sci USA* **111**, 17272–17277.
- Hobson MI, Green CJ and Terenghi G (2000) VEGF enhances intraneural angiogenesis and improves nerve regeneration after axotomy. *J Anat* **197**, 591–605.
- Höke A, Sun HS, Gordon T and Zochodne DW (2001) Do denervated peripheral nerve trunks become ischemic? The impact of chronic denervation on vasa nervorum. *Exp Neurol* **172**, 398–406.
- Kim BS, Yoo JJ and Atala A (2004) Peripheral nerve regeneration using acellular nerve grafts. *J Biomed Mater Res A* **68**, 201–209.
- Koch S, Tugues S, Li X, Gualandi L and Claesson-Welsh L (2011) Signal transduction by vascular endothelial growth factor receptors. *Biochem J* **437**, 169–183.
- Lindholm T, Risling M, Carlstedt T, Hammarberg H, Wallquist W, Cullheim S and Sköld MK (2017) Expression of semaphorins, neuropilins, VEGF, and tenascins in rat and human primary sensory neurons after a dorsal root injury. *Front Neurol* **8**, 49. doi: 10.3389/fneur.2017.00049.
- Mackenzie F and Ruhrberg C (2012) Diverse roles for VEGF-A in the nervous system. *Development* **139**, 1371–1380.
- Muratori L, Gnani S, Fregnan F, Mancardi A, Raimondo S, Perroteau I and Geuna S (2018) Evaluation of vascular endothelial growth factor (VEGF) and its family member expression after peripheral nerve regeneration and denervation. *Anat Rec (Hoboken)* **301**, 1646–1656.
- Olsson AK, Dimberg A, Kreuger J and Claesson-Welsh L (2006) VEGF receptor signalling – in control of vascular function. *Nat Rev Mol Cell Biol* **7**, 359–371.
- Pan Z, Fukuoka S, Karagianni N, Guaiquil VH and Rosenblatt MI (2013) Vascular endothelial growth factor promotes anatomical and functional recovery of injured peripheral nerves in the avascular cornea. *FASEB J* **27**, 2756–2767.
- Pereira Lopes FR, Martin PK, Frattini F, Biancalana A, Almeida FM, Tomaz MA, Melo PA, Borojevic R, Han SW and Martinez AM (2013) Double gene therapy with granulocyte colony-stimulating factor and vascular endothelial growth factor acts synergistically to improve nerve regeneration and functional outcome after sciatic nerve injury in mice. *Neuroscience* **230**, 184–197.
- Sondell M, Lundborg G and Kanje M (1999) Vascular endothelial growth factor stimulates Schwann cell invasion and neovascularization of acellular nerve grafts. *Brain Res* **846**, 219–228.
- Sondell M, Lundborg G and Kanje M (1999) Vascular endothelial growth factor has neurotrophic activity and stimulates axonal outgrowth, enhancing cell survival and Schwann cell proliferation in the peripheral nervous system. *J Neurosci* **19**, 5731–5740.
- Vempati P, Popel AS and Mac Gabhann F (2014) Extracellular regulation of VEGF: isoforms, proteolysis, and vascular patterning. *Cytokine Growth Factor Rev* **25**, 1–19.
- Yamada Y, Ohazama A, Maeda T and Seo K (2018) The Sonic Hedgehog signaling pathway regulates inferior alveolar nerve regeneration. *Neurosci Lett* **671**, 114–119.
- Zupanc HRH, Alexander PG and Tuan RS (2017) Neurotrophic support by traumatized muscle-derived multipotent progenitor cells: Role of endothelial cells and vascular endothelial growth factor-A. *Stem Cell Res Ther* **8**, 226.